Optical Probing of Ultrafast Electronic Decay in Bi and Sb with Slow Phonons

J. J. Li,[1] J. Chen,[2] D. A. Reis,[2,3] S. Fahy,[4] and R. Merlin[1]

[1]*Department of Physics, University of Michigan, Ann Arbor, MI 48109-1040, USA*
[2]*Stanford PULSE Institute, SLAC National Accelerator Laboratory, Menlo Park, CA 94025, USA*
[3]*Departments of Photon Science and Applied Physics, Stanford University, Stanford, CA 94309, USA*
[4]*Tyndall National Institute and Department of Physics, University College, Cork, Ireland*

Illumination with laser sources leads to the creation of excited electronic states of particular symmetries, which can drive isosymmetric vibrations. Here, we use a combination of ultrafast stimulated and cw spontaneous Raman scattering to determine the lifetime of A_{1g} and E_g electronic coherences in Bi and Sb. Our results both shed new light on the mechanisms of coherent phonon generation and represent a novel way to probe extremely fast electron decoherence rates. The E_g state, resulting from an unequal distribution of carriers in three equivalent band regions, is extremely short lived. Consistent with theory, the lifetime of its associated driving force reaches values as small as 2 (6) fs for Bi (Sb) at 300 K.

Measurements of excited-state lifetimes have a rich history. Recent advances in ultrafast laser science have made it possible to determine time intervals of a few attoseconds [1], considerably shorter than those that can be measured with, e.g., recoil Doppler-shift methods in nuclear physics [2] or vertex reconstruction in particle physics [3]. All these techniques are direct in that they are based either on measurements of the speed and distance traveled by the decaying particle or use tools that operate in time scales shorter than the lifetime probed. Here, we describe a novel, indirect method which allows lifetime determination in the femtosecond range using vibrations of periods that are ~ 100 times longer. Our approach relies on a comparison between the amplitude of coherent phonon oscillations in time-domain (TD) experiments [4–6] and the cross section of spontaneous Raman scattering (RS). Its scope spans lifetime studies in solids and molecules [7]. The results also help elucidate long-standing questions about the processes responsible for coherent phonon generation, particularly the subtle differences between stimulated RS [8,9] and the mechanism known as displacive excitation of coherent phonons (DECP) [10–12].

Typically TD experiments on coherent vibrations involve two light pulses: the pump, which makes the ions oscillate coherently, and the probe, which is sensitive to the changes these vibrations produce in the optical constants [4–6]. Here we are interested in the effects due to excited-state decay in the excitation of opaque materials. The electron-mediated interaction between a classical electromagnetic field and a single optical phonon is described by the Hamiltonian [8,9,12]

$$\hat{H} = \tfrac{1}{2}(P_{\mathbf{q}}^2 + \Omega_{\mathbf{q}}^2 Q_{\mathbf{q}}^2) - \hat{\bar{\Xi}}_{\mathbf{q}} Q_{\mathbf{q}} - \hat{\Delta} \cdot \mathbf{E}(t) + \hat{V}. \quad (1)$$

Here, $\mathbf{E}(t)$ is the electric field at time t; $\hat{\Delta}$ is the dipole moment of the electronic system; $\hat{V}$ contains both the interaction between electrons and between electrons and

other phonons; and $Q_{\mathbf{q}}$ and $P_{\mathbf{q}}$ are the coordinate and momentum of the mode of wave vector $\mathbf{q}$ and frequency $\Omega_{\mathbf{q}}$. As discussed in Ref. [5], the symmetry of the phonons to which light couples must match one of the Raman-allowed representations. The two Raman modes in Bi and Sb belong to representations A_{1g} and E_g of the point group $\bar{3}m$; the corresponding displacements are shown in Fig. 1. The term $\hat{\bar{\Xi}}_{\mathbf{q}} Q_{\mathbf{q}}$ represents the coupling of the mode with the electrons, $\hat{\bar{\Xi}}_{\mathbf{q}} = N^{-1/2} \sum_{mn,\mathbf{k}} \xi_{mn}^{\mathbf{kq}} c_{m,\mathbf{k}}^{\dagger} c_{n,\mathbf{k}-\mathbf{q}}$, where N is the number of cells, $c_{m,\mathbf{k}}^{\dagger}$ and $c_{m,\mathbf{k}}$ are electron creation and annihilation operators for the state of wave vector $\mathbf{k}$ in band m, and $\xi_{mn}^{\mathbf{kq}}$ are deformation potentials.

Ignoring phonon decay [9,12],

$$\frac{d^2}{dt^2}\langle Q_{\mathbf{q}}\rangle + \Omega_{\mathbf{q}}^2\langle Q_{\mathbf{q}}\rangle = F_{\mathbf{q}} \equiv \langle \hat{\bar{\Xi}}_{\mathbf{q}}\rangle, \quad (2)$$

where $\langle \dots \rangle$ denotes the expectation value. The driving force $F_{\mathbf{q}}$ is associated with a weighted charge-density
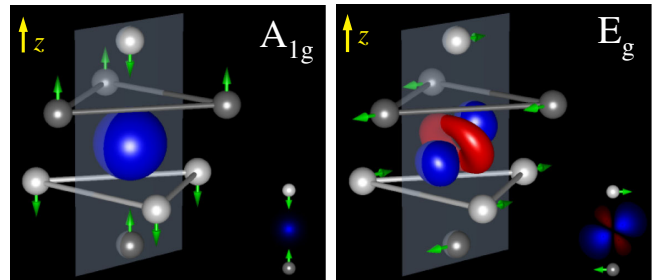

FIG. 1 (color online). Schematic representation of the ionic displacements and the corresponding isosymmetric charge fluctuations that couple to the A_{1g} and E_g modes. Separate (blue and red) lobes of the charge fluctuations indicated correspond to charge densities of opposite sign. The trigonal axis is along z. The smaller drawings on the bottom right show a cross section defined by the gray planes in the main figures.

fluctuation with the same symmetry as the phonon. A schematic representation of the fluctuations that drive the two Raman-allowed modes in Bi and Sb is also shown in Fig. 1. These charge configurations represent a Raman-type coherence involving, in general, diagonal as well as off-diagonal terms of the form $\langle c_{m,\mathbf{k}}^{\dagger} c_{n,\mathbf{k}-\mathbf{q}} \rangle$ as opposed to that of the induced carrier population, which depends on the number of photoexcited electrons $\nu_{n,\mathbf{k}}^{e} = \langle c_{n,\mathbf{k}}^{\dagger} c_{n,\mathbf{k}} \rangle$ and holes $\nu_{n,\mathbf{k}}^{h} = \langle c_{n,\mathbf{k}} c_{n,\mathbf{k}}^{\dagger} \rangle$, which affects only modes at $\mathbf{q} = 0$. $F_{\mathbf{q}}$ is determined by the Raman tensor associated with the coherent phonon generation, $\pi_{\mu\nu}^{R}$. In the limit $\mathbf{q} \rightarrow 0$ and including decay of the electron-hole excitation due to $\hat{V}$ [9,13],

$$\pi_{\mu\nu}^{R}(\omega_1, \omega_2) \approx \frac{\xi}{4\pi\hbar} \left[\frac{\epsilon(\omega_1) - \epsilon^*(\omega_2)}{\omega_1 - \omega_2 + i\Gamma} \right] C_{\mu\nu}. \quad (3)$$

Here, ξ is an average of the difference between the electron and hole band deformation potentials, $C_{\mu\nu}$ is a tensor whose constant elements reflect the phonon symmetry, and we assume that the decay of off-diagonal elements satisfies $\gamma_{n,m} = \gamma_n + \gamma_m \approx \Gamma$. If the permittivity does not vary much with frequency,

$$F(t) \approx \frac{N^{1/2} v_c \xi}{\hbar} \, \text{Im}[\epsilon(\omega_c)] \int_{-\infty}^{t} e^{-\Gamma(t-t')} |E(t')|^2 dt', \quad (4)$$

where v_c is the cell volume and ω_c is the central frequency of the pump pulse. The Fourier transform of (4) differs from Eq. (10) of Ref. [9] in that it explicitly includes decay. A similar expression was given in [13] in the context of the DECP model through the decay of the diagonal terms in (2). Up to a numerical factor of order 1, at times $t \gg \tau$ and for $\Omega\tau \ll 1$ (τ is the pulse width)

$$Q(t) \sim \frac{N^{1/2} v_c \tilde{\xi} \text{Im}[\epsilon(\omega_c)] |E_0|^2 \tau}{\hbar\Omega^2}$$
$$\times \left[\frac{e^{-\Gamma t}}{\sqrt{1 + \Gamma^2/\Omega^2}} - \cos(\Omega t + \phi) \right]. \quad (5)$$

Here, $\tan\phi = \Gamma/\Omega$, E_0 is the peak electric field, and we introduce $\tilde{\xi} = \xi(1 + \Gamma^2/\Omega^2)^{-1/2}$, which plays the role of an effective electron-phonon coupling energy. Hence, electronic decay leads to a decrease of the amplitude by a factor $(1 + \Gamma^2/\Omega^2)^{-1/2}$ and a modification of the phase of the coherent oscillations. As shown later, the decay-induced reduction in the amplitude allows one to determine Γ from a comparison between RS and TD results.

The coherent vibrations generated by the pump cause oscillatory changes in the optical constants that can be measured by monitoring concomitant changes in the reflectivity or transmission of the probe pulse. The latter process relates to the Raman contribution to the polarization [5,9]. Under the same assumptions as (3), the conventional Raman susceptibility tensor is

$$\chi_{\mu\nu}^{R}(\omega, \omega - \Omega) \approx \frac{\xi}{4\pi\hbar} \left[\frac{\epsilon(\omega) - \epsilon(\omega - \Omega)}{\Omega} \right] C_{\mu\nu}. \quad (6)$$

As noted in [9], in the absence of absorption $\chi_{\mu\nu}^{R} = \pi_{\mu\nu}^{R}$. Otherwise, and even in the limit $\gamma \rightarrow 0$ considered in [8,9], the two Raman tensors exhibit substantial differences [9]. Decay appears twice in (3), once in the permittivity and a second time to account for the fact that, in the presence of absorption, vibrations couple to real charge fluctuations that have a finite lifetime. Instead, decay manifests itself only once in the conventional Raman tensor, (6), through the permittivity. The amplitude of the coherent-phonon-induced change in the complex refractive index is

$$\delta n = \frac{2\pi}{n} \chi^{R} Q \approx \text{Im}\left(\epsilon \frac{dn}{d\omega} \right) \Big|_{\omega_c} \frac{\xi\tilde{\xi}|E_0|^2 \tau v_c}{2\pi\hbar^2\Omega^2}. \quad (7)$$

As the integrated intensity for RS is [14]

$$S \propto |\xi|^2 (n_B + 1)/\Omega, \quad (8)$$

where n_B is the Bose thermal factor, it is apparent that $\tilde{\xi}$ and, therefore, Γ can be gained from a combination of TD and spontaneous RS data.

Spontaneous Raman and ultrafast time-domain measurements were performed on a single crystal of Sb and a $\sim$100-nm-thick single-crystal film of Bi grown on a c-cut sapphire substrate, both with the trigonal z axis perpendicular to the surface. The pump-induced relative change in the reflectivity of the probe, $\Delta R/R = 2[\delta n/(n^2 - 1) + \text{c.c.}]$ was measured as a function of the time delay between the two pulses. Our detection scheme is sensitive to the pump-induced xy birefringence, which made it possible to separate the weaker E_g oscillations from those of the dominant A_{1g} mode [8]. As a source, we used a mode-locked Ti-sapphire laser providing 70 fs pulses centered at 800 nm with a repetition rate of 250 kHz. The pump (probe) pulse was focused onto a spot of radius 100 (40) μm; the average power was 2.2 (0.5) mW. Spontaneous RS experiments were performed with 30 mW cw Ti:sapphire laser at 780 nm in the backscattering geometry $z(x, x)\bar{z}$. Typical measurements at 10 and 300 K are shown in Fig. 2.

The data show two, high- and low-frequency features corresponding to the A_{1g} and E_g phonons, which obey the expected Raman selection rules [8]. In both substances, the modes exhibit an increase (decrease) in linewidth (frequency) with increasing temperature, T, which is similar to what is found in many materials, likely, a manifestation of anharmonic decay. Consistent with our low power densities, corresponding values from cw spontaneous RS and TD traces agree well with each other, and with early Raman work [15,16]. The spontaneous cross sections show a relatively weak T dependence, in agreement with a previous report [15]. Unlike the spontaneous RS results,
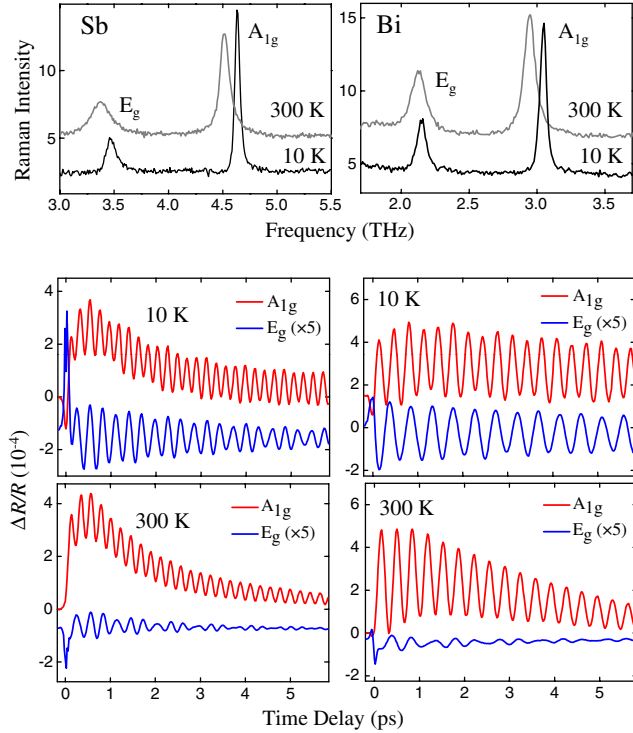
FIG. 2 (color online). Spontaneous Raman and pump-probe data for Bi and Sb at 10 and 300 K. Spontaneous Raman spectra are shown in the top two panels; intensity units are arbitrary and the geometry is $z(x,x)\bar{z}$. The bottom two panels show pump-probe differential reflectivity data in a geometry that is sensitive to the pump-induced xy birefringence. High and low frequency oscillations and spectral features are due, respectively, to the A_{1g} and E_g modes. The TD A_{1g} traces also show a slowly decaying electronic background. Plots have been shifted vertically for clarity.

FIG. 3 (color online). Temperature dependence of the ratio between effective electron-phonon coupling for the A_{1g} and E_g modes for spontaneous RS and for TD experiments extracted from Eqs. (7) and (8). Lines are fits to the data.

however, and in contrast to the behavior of the A_{1g} mode, whose amplitude is nearly independent of temperature, the initial E_g amplitude shows a pronounced decrease with increasing T.

The data in Fig. 3, comparing electron-phonon coupling ratios derived from spontaneous RS and TD experiments, emphasize the differences between the two sets of results for the E_g mode. In spontaneous RS, the average deformation potential difference ξ gives a direct measure of the effective coupling; it can be gained from a determination of the absolute cross section [17]. As shown in Fig. 3, and consistent with Ref. [15], the deformation potential ratio, $g_{RS} \equiv |\xi(A_{1g})/\xi(E_g)|$ obtained from the expression for the integrated intensity, (8), is nearly T independent in both substances. On the other hand, given that $\Delta R \propto \delta n \propto \xi\tilde{\xi}/\Omega^2$, the ratio of the effective coupling for pump-probe experiments is $g_{PP} \equiv |\sqrt{\tilde{\xi}\xi(A_{1g})/\tilde{\xi}\xi(E_g)}|$; see (7). In the TD case, the effective coupling ratio increases with increasing T, reflecting the strong decrease in the E_g amplitude, more so in Bi than in Sb. Since $\xi = \tilde{\xi}$ in the
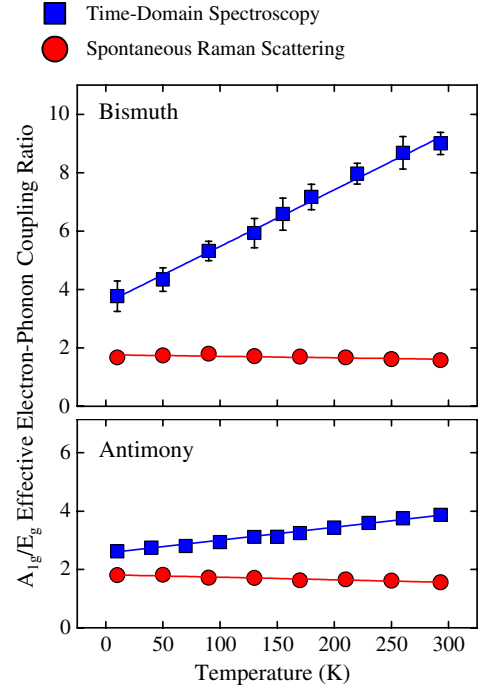
absence of electronic decay, we interpret the large differences in the effective coupling ratios, particularly at high temperatures, as a clear indication of electronic-decay effects on the E_g oscillations. In determining the effective coupling constants, the initial pump-probe oscillation amplitudes were multiplied by the Gaussian factor $\exp(\Omega^2\tau^2/2)$ [4,5]. This correction, accounting for the finite pump and probe pulse duration, amounts to a factor of less than 10% (20%) for Bi (Sb).

As mentioned above, the amplitude of the A_{1g} oscillations does not depend much on T. From these results, the T dependence of the RS cross sections, the decay of the electronic background, and the available optical data [18], we conclude that $\Gamma \ll \Omega$ for the A_{1g} phonon. Using this and the deformation potential ratios from the spontaneous RS data, we determine the lifetime of the E_g driving force, $1/\Gamma(E_g) \approx \Omega(E_g)^{-1}(g_{PP}^4/g_{RS}^4 - 1)^{-1/2}$. Results are shown in Fig. 4 (note that the lifetime of the electronic coherence is $2/\Gamma$). Since most of the channels available for scattering of highly excited electrons and holes from other electrons or holes are unaffected by temperature changes of the order of the phonon frequency, we ascribe the decay to electron-phonon interaction. This attribution is supported by the facts that (i) the dependence of the lifetime on temperature closely follows that of the phonon occupation, which appears in decay processes involving phonon emission and absorption by photoexcited carriers, and that (ii) values $\Theta(\text{Bi}) = 8.9$ meV and $\Theta(\text{Sb}) = 19.4$ meV
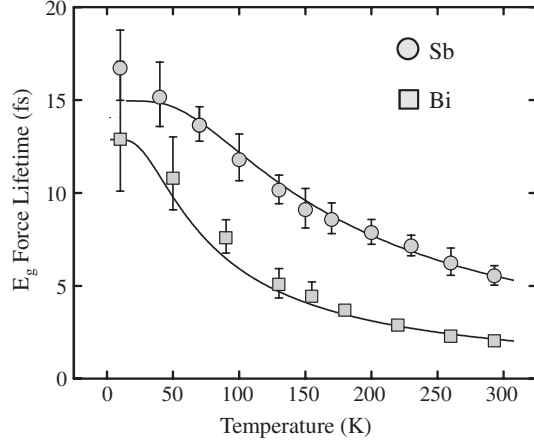
FIG. 4.   Temperature dependence of the E_g force lifetime, $1/\Gamma$ (the electronic lifetime is $2/\Gamma$). Curves involve fits of Γ to $\Gamma_0[2n_B(\Theta) + 1]$, where Γ_0 is the low temperature decay rate and Θ is the Debye energy.

from the fits are in excellent agreement with the Debye energies of Bi (10 meV) and Sb (17 meV) [19].

The real-space E_g charge-density fluctuation depicted in Fig. 1 can be shown to reflect an unbalanced occupation of states in regions of the Brillouin zone that are equivalent under threefold rotations about the trigonal axis. This difference in occupation arises in the initial photoexcitation process because of the polarization dependence of the optical transition dipole matrix elements. Momentum scattering will cause these differences to decay at the rate γ_M. Assuming that electron-phonon scattering is the dominant mechanism for momentum relaxation, Sheu *et al.* [20] show that, within a simple two-temperature model with parabolic bands and classical phonons, γ_M and the rate of thermal equilibration between the electronic plasma and the lattice, γ_L, are related by

$$\gamma_M \approx \left(\frac{3k_B T_p}{\Sigma_L}\right)\left(\frac{k_B T_L}{\Sigma_L}\right)\gamma_L \gg \gamma_L,$$

where k_B is the Boltzmann constant, Σ_L is the typical energy of phonons involved in the electron-phonon scattering process, T_p is the electron-hole plasma temperature ($3k_B T_p$ is initially comparable to the incident photon energy ~ 1.5 eV), and T_L is the lattice temperature. The rate of thermal equilibration between the lattice and the electronic plasma has been estimated to be ~ 2 ps [20,21]. Assuming that Σ_L is equal to the Debye energy, we obtain the estimates of the room temperature relaxation time $1/\gamma_M \approx 5$ fs (Bi) and 10 fs (Sb), in good agreement with the our measured lifetimes of the E_g forces.

As by (5), stimulated RS theory predicts roughly the same decay-induced reduction of the amplitude for all Raman-allowed modes, thus raising the question as to why the electronic decay, which manifests itself in the large T dependence of the E_g amplitude, hardly affects A_{1g}. To address this point, consider the RS force for the

mode at $\mathbf{q} = 0$ (similar arguments apply to the other modes for which the charge-density fluctuation varies sinusoidally from cell to cell). We introduce the scattering probability $P^{e,h}(n'\mathbf{k}', n\mathbf{k}; t)$, which equals the probability that an electron or hole in state $|n, \mathbf{k}\rangle$ has scattered to state $|n', \mathbf{k}'\rangle$ after time t, so that

$$F_0(t) \approx N^{-1/2}\sum_{nn',\mathbf{kk}'}\xi_{nn'}[P^e(n'\mathbf{k}', n\mathbf{k}; t)\nu^e_{n,\mathbf{k}}$$
$$- P^h(n'\mathbf{k}', n\mathbf{k}; t)\nu^h_{n,\mathbf{k}}].$$

After scattering, the perturbation-theory RS expression, (4), no longer applies. Since the principal electron scattering mechanism is by phonons, with scattering wave vectors throughout the Brillouin zone, after a few scattering events both electrons and holes will be nearly uniformly distributed over the energy shell, where $E(n'\mathbf{k}')$ lies within a few times Σ_L of $E(n\mathbf{k})$. As the redistribution produces a uniform density fluctuation, the force on the A_{1g} phonon, albeit no longer of the RS-type, remains roughly unchanged. That is, for $t \gg 1/\gamma_M$,

$$F_0 \approx N^{-1/2}\left(\langle\xi_e\rangle\sum_{n,\mathbf{k}}\nu^e_{n,\mathbf{k}} - \langle\xi_h\rangle\sum_{n,\mathbf{k}}\nu^h_{n,\mathbf{k}}\right) = N^{-1/2}\xi\nu_T,$$

where ν_T is the total number of photoexcited electrons (or holes). Thus the A_{1g} phonon force decays with the lifetime of the photoexcited carriers.

The above description of the A_{1g} excitation is that of the DECP mechanism, originally introduced to explain coherent oscillations of fully symmetric modes [11]. Accordingly, we attribute the observation of large A_{1g} oscillations at high temperatures to DECP effects that persist because of the large lifetime of the population of photoexcited carriers. Further, the data in Fig. 3 clearly show that a DECP component remains at low temperatures where the strengths of A_{1g} RS and DECP contributions are comparable in both substances. While an analogous DECP force could be envisioned for the $\mathbf{q} = 0$ E_g mode, it would only matter if the scattering rate for very small wave vector transfers were much larger than γ_M, a possibility that is highly unlikely. More generally, we note that, within the context of TD experiments, the DECP mechanism matters only in substances for which the light penetration depth is small compared with the wavelength. In these cases, probe scattering is dominated by surface effects regardless of the wave vector of the charge fluctuation [5].

[1] M. Schultze *et al.*, Science **328**, 1658 (2010).
[2] A. E. Blaugrun, Nucl. Phys. **88**, 501 (1966).

[3] R. H. Perkins, *Introduction to High Energy Physics* (Cambridge University Press, Cambridge, England, 2000), 4th ed.

[4] L. Dhar, J. A. Rogers, and K. A. Nelson, Chem. Rev. **94**, 157 (1994).

[5] R. Merlin, Solid State Commun. **102**, 207 (1997).

[6] T. Dekorsy, G. C. Cho, and H. Kurz, in *Light Scattering in Solids VIII*, edited by M. Cardona and G. Güntherodt (Springer, Berlin, 2000).

[7] C. E. Crespo-Hernández, B. Cohen, P. M. Hare, and B. Kohler, Chem. Rev. **104**, 1977 (2004).

[8] G. A. Garrett, T. F. Albrecht, J. F. Whitaker, and R. Merlin, Phys. Rev. Lett. **77**, 3661 (1996).

[9] T. E. Stevens, J. Kuhl, and R. Merlin, Phys. Rev. B **65**, 144304 (2002).

[10] T. K. Cheng, J. Vidal, H. J. Zeiger, G. Dresselhaus, M. S. Dresselhaus, and E. P. Ippen, Appl. Phys. Lett. **59**, 1923 (1991).

[11] H. J. Zeiger, J. Vidal, T. K. Cheng, E. P. Ippen, G. Dresselhaus, and M. S. Dresselhaus, Phys. Rev. B **45**, 768 (1992).

[12] A. V. Kuznetsov and C. J. Stanton, Phys. Rev. Lett. **73**, 3243 (1994).

[13] D. M. Riffe and A. J. Sabbah, Phys. Rev. B **76**, 085207 (2007).

[14] W. Hayes and R. Loudon, *Scattering of Light by Crystals* (Wiley, New York, 1978), p. 31.

[15] J. B. Renucci, W. Richter, M. Cardona, and E. Schönherr, Phys. Status Solidi B **60**, 299 (1973).

[16] J. Höhne, U. Wenning, H. Schulz, and S. Höfner, Z. Phys. B **27**, 297 (1977).

[17] *Light Scattering in Solids II*, edited by M. Cardona and G. Güntherdodt (Springer, Berlin, 1982), Chap. 2.

[18] M. Cardona and D. L. Greenaway, Phys. Rev. **133**, A1685 (1964).

[19] P. Fischer, I. Sosnowska, and M. Szymanski, J. Phys. C **11**, 1043 (1978).

[20] Y. M. Sheu, Y. J. Chien, C. Uher, S. Fahy, and D. A. Reis (unpublished).

[21] G. Sciaini, M. Harb, S. G. Kruglik, T. Payer, C. T. Hebeisen, F.-J. Meyer zu Heringdorf, M. Yamaguchi, M. Horn-von Hoegen, R. Ernstorfer, and R. J. D. Miller, Nature (London) **458**, 56 (2009).